
Generative Pretraining for Black-Box Optimization

Siddarth Krishnamoorthy *
UCLA
siddarthk@cs.ucla.edu

Satvik Mehul Mashkaria *
UCLA
satvikm@cs.ucla.edu

Aditya Grover
UCLA
adityag@cs.ucla.edu

Abstract

Many problems in science and engineering involve optimizing an expensive black-box function over a high-dimensional space. For such black-box optimization (BBO) problems, we typically assume a small budget for online function evaluations, but also often have access to a fixed, offline dataset for pretraining. Prior approaches seek to utilize the offline data to approximate the function or its inverse but are not sufficiently accurate far from the data distribution. We propose **Black-box Optimization Transformer** (BOOMER), a generative framework for pretraining black-box optimizers using offline datasets. In BOOMER, we train an autoregressive model to imitate trajectory runs of implicit black-box function optimizers. Since these trajectories are unavailable by default, we develop a simple randomized heuristic to synthesize trajectories by sorting random points from offline data. We show theoretically that this heuristic induces trajectories that mimic transitions from diverse low-fidelity (exploration) to high-fidelity (exploitation) samples. Further, we introduce mechanisms to control the rate at which a trajectory transitions from exploration to exploitation, and use it to generalize outside the offline data at test-time. Empirically, we instantiate BOOMER using a casually masked Transformer [1, 2] and evaluate it on Design-Bench [3], where we rank the best on average, outperforming state-of-the-art baselines.

1 Introduction

Many fundamental problems in science and engineering, ranging from the discovery of drugs and materials to the design and manufacturing of hardware technology, require optimizing an expensive black-box function in a large search space [4, 5, 6, 7]. The key challenge here is that evaluating and optimizing such a black-box function is typically expensive, as it often requires real-world experimentation and exploration of a high-dimensional search space.

Fortunately, for many such black-box optimization (BBO) problems, we often have access to an offline dataset of function evaluations. Such an offline dataset can greatly reduce the budget for online function evaluation.

One natural approach for offline BBO would be to train a surrogate (forward) model that approximates the black-box function using the offline data. Once learned, we can perform gradient ascent on the input space to find the optimal point. Unfortunately, this method does not perform well in practice because the forward model fails to generalize to points outside the offline dataset or proposes invalid points outside the support of the black-box function, all of which can cause the model to incorrectly give sub-optimal points a high score (see Figure 1). To mitigate this issue, COMs [8] learns a forward mapping that penalizes high scores on points outside the dataset, but this can have the opposite effect of not being able to explore high fidelity points that are far from the dataset. Further, another class of recent approaches [9, 10, 11] propose a conditional generative approach that learns an inverse mapping function values to the points. For effective generalization, such a mapping needs to be highly

*Equal contribution

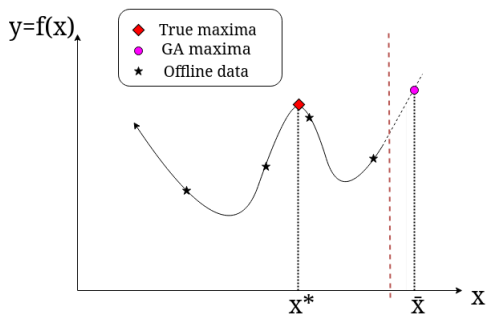


Figure 1: Example of offline BBO on toy 1D problem. Here, the domain ends at the red dashed line. Thus, the correct optimal value is x^* , whereas gradient ascent on the fitted function will output out of the domain point \bar{x} .

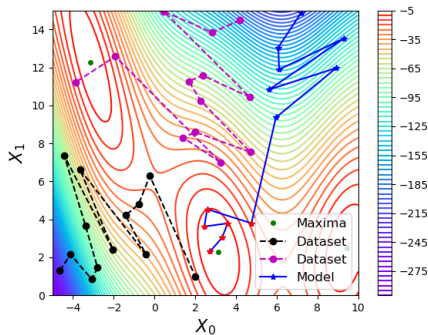


Figure 2: Example trajectory on the 2D-Branin function. The two dotted lines denote the trajectories in our offline dataset, and the solid line refers to our model trajectory, with blue points showing exploration and red points showing exploitation.

multimodal and non-convex for high-dimensional functions, which in itself presents a challenge for current approaches.

We propose **Black-box Optimization Transformer (BOOMER)**, a new generative framework for pretraining black-box optimizers on offline datasets. Instead of approximating the surrogate function (or its inverse), we seek to learn the explore-exploit dynamics of black-box optimizers using an autoregressive sequence model. Naively, this would require access to several trajectory runs of different black-box optimizers, which is expensive or even impossible in many cases. Our key observation is that we can use our offline dataset to synthesize trajectories that have similar properties to rollouts of an online algorithm for BBO (e.g., bandits [12, 13], Bayesian optimization [14]). In particular, we use a heuristic to sample fixed-length trajectories of offline points that are monotonic in their function values. Such trajectories intuitively emphasize an exploration phase early on – encoded by poor but diverse offline points; followed by an exploitation phase – encoded by high quality offline points concentrated around the empirically observed optima in the offline dataset.

Further, we augment every offline point in our trajectories with a *regret budget*, which is defined as the cumulative regret of the trajectory starting at the current point until the end of the trajectory. For low regret budgets, we emphasize exploitation over exploration and vice versa. Thus, at test time, BOOMER can generate candidate points outside the offline dataset by rolling out a trajectory with a low regret budget. Figure 2 shows an illustration of how trajectories generated by BOOMER can achieve lower regret than the trajectories used to train it.

We evaluate our method on several real world tasks in the Design-Bench [3] dataset. These tasks are based on real world problems such as robot morphology optimization, DNA sequence optimization and optimizing superconducting temperature of materials, all of which require searching over a high-dimensional space. We achieve a normalized mean score of **0.772** and an average rank of **2.4** across all datasets, outperforming the next best baseline, which achieves a rank of 3.7.

2 Pretraining Black-Box Optimizers via BOOMER

2.1 Problem Statement

Let $f : \mathcal{X} \rightarrow \mathbb{R}$ be a black-box function, where $\mathcal{X} \subseteq \mathbb{R}^d$ is an arbitrary d -dimensional domain. In black-box optimization (BBO), we are interested in finding the point \mathbf{x}^* that maximizes f :

$$\mathbf{x}^* \in \operatorname{argmax}_{\mathbf{x} \in \mathcal{X}} f(\mathbf{x}) \quad (1)$$

Typically, f is expensive to evaluate and we do not assume direct access to it during training. Instead, we have access to an offline dataset of N previous function evaluations $\mathcal{D} = \{(\mathbf{x}_1, y_1), \dots, (\mathbf{x}_N, y_N)\}$, where $y_i = f(\mathbf{x}_i)$. For evaluating a black-box optimizer post-training, we

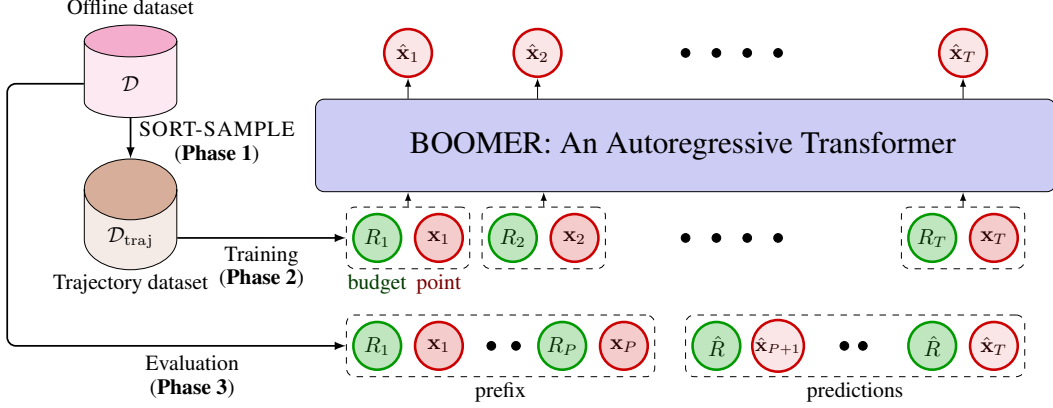


Figure 3: Schematic for BOOMER. In Phase 1, we construct a trajectory dataset $\mathcal{D}_{\text{traj}}$ using SORT-SAMPLE. In Phase 2, we learn an autoregressive model for $\mathcal{D}_{\text{traj}}$. In Phase 3, we condition the model on an offline prefix sequence and unroll it further to obtain candidate proposals $\hat{\mathbf{x}}_{P+1:T}$.

allow it to query the black-box function f for a small budget of Q queries and output the point with the best function value obtained. This protocol follows prior works in offline BBO [8, 3, 9, 10, 11].

Overview of BOOMER We illustrate our proposed framework for offline BBO in Figure 3 and Algorithm 1. BOOMER consists of 3 sequential phases: trajectory construction, autoregressive modelling, roll-out evaluation. In Phase 1 (Section 2.2), we transform the offline dataset \mathcal{D} into a trajectory dataset $\mathcal{D}_{\text{traj}}$. This is followed by Phase 2 (Section 2.3), where we train an autoregressive model on $\mathcal{D}_{\text{traj}}$. Finally, we evaluate the model by rolling out Q candidate points in Phase 3 (Section 2.4).

Algorithm 1 BOOMER

- Input** Offline dataset \mathcal{D} , Evaluation Regret Budget \hat{R} , prefix length P , Query budget Q , trajectory length T , num_trajs, K , τ , N_B , model hyper-parameters
Output A set of proposed candidate points \mathbf{X} with the constraint $|\mathbf{X}| \leq Q$
- 1: \triangleright **Phase 1:** SORT-SAMPLE
 - 2: Construct bins $\{B_1, \dots, B_{N_B}\}$ from \mathcal{D} , each bin covering equal y -range, as described in 2.2
 - 3: Calculate the scores $(n_1, n_2, \dots, n_{N_B})$ for each bin using K and τ
 - 4: $\mathcal{D}_{\text{traj}} \leftarrow \phi$
 - 5: **for** $i = 1, \dots, \text{num_trajs}$ **do**
 - 6: Uniformly randomly sample n_i points from B_i and concatenate them to construct \mathcal{T}
 - 7: Sort \mathcal{T} in the ascending order of the function value
 - 8: Represent \mathcal{T} as $(R_1, \mathbf{x}_1, R_2, \mathbf{x}_2, \dots, R_T, \mathbf{x}_T)$, following equation 3, and append \mathcal{T} to $\mathcal{D}_{\text{traj}}$
 - 9: **end for**
 - 10: \triangleright **Phase 2:** Training
 - 11: Train the model g_θ to maximize the log-likelihood of $\mathcal{D}_{\text{traj}}$ using the loss in equation 4
 - 12: \triangleright **Phase 3:** Evaluation
 - 13: Construct a trajectory \mathcal{T}' from \mathcal{D} following Phase 1, and delete the last $T - P$ points
 - 14: Calculate R_t and feed (R_t, \mathbf{x}_t) to g_θ sequentially, $\forall t = 1, \dots, P$
 - 15: Roll-out g_θ autoregressively while feeding $R_t = \hat{R}, \forall t = P + 1, \dots, T$
 - 16: \mathbf{X} is the set of last $\min(Q, T - P)$ rolled-out points.
-

2.2 Phase 1: Constructing Explore-Then-Exploit Trajectories

In the online setting, the predominant approaches to BBO [14, 12] rely on balancing exploration and exploitation within a small budget. Early on, these approaches expend their budget in querying a diverse set of points, i.e., exploration. Such an exploration is usually followed by an exploitation phase, where the optimizers zooms in on regions with promising points.

Our key motivation in BOOMER is to train a model to mimic the aforementioned sequential behavior of the online black-box optimizers. However, the key difficulty is that we do not have the ability to generate trajectories by actively querying the black-box function during training. In BOOMER, we overcome this difficulty by synthesizing trajectories purely from an offline dataset based on two guiding desiderata. Our first guiding principle is that each trajectory should exhibit an exploration phase followed by exploitation, akin to an online BBO optimizer. Secondly, the construction of these trajectories should scale to high-dimensional data points and large offline datasets. We refer to trajectories that satisfy the above desiderata as explore-then-exploit trajectories.

Explore-Then-Exploit via Sorting We propose to satisfy the above desiderata in BOOMER by following a sorting heuristic. Specifically, given a set of T offline points, we construct an explore-then-exploit trajectory of length T by simply sorting the points in ascending order from low to high function values. Intuitively, we expect the low function values at the beginning of a trajectory to belong to a more diverse region of the search space and thus reflect an exploration phase. Similarly, the high function values indicate an exploitation phase. We can formalize this intuition further by considering continuously differentiable black-box functions. We consider 1D functions with certain assumptions here for simplicity, and defer the discussion for more general functions in higher dimensions to Appendix A. First, we define a notion of ϵ -high points.

Definition 1. ϵ -high values. Let the range of f be denoted as $[y_{min}, y_{max}]$. Then, a function value y in this range is ϵ -high if $y \geq y_{min} + \epsilon(y_{max} - y_{min})$.

Intuitively, the above definition implies that y is ϵ -high if it is in the top $1 - \epsilon$ fraction of the range of f . The following result characterizes the relative diversity of regions consisting of ϵ -high points.

Proposition 1. Let $f : [a, b] \rightarrow \mathbb{R}$, $a, b \in \mathbb{R}$, be a real-valued, continuous and differentiable function such that the $f(a)$ and $f(b)$ are not ϵ -high. Let $H \subseteq [a, b]$ be a Lebesgue-measurable set of x values for which $f(x)$ is ϵ -high, with $\epsilon > 0.5$. Let $H^c = [a, b] \setminus H$. Without loss of generality, let's assume that $f(a) \leq f(b)$. If the Lipschitz constant L of f is upper bounded by

$$\frac{2(\epsilon(y_{max} - y_{min}) + y_{min} - f(a))}{b - a}, \quad (2)$$

then $|H| < |H^c|$, where $|\cdot|$ denotes volume of a set w.r.t. the Lebesgue Measure.

The above proposition characterizes functions for which the volume (i.e., sum of interval lengths in 1D) occupied by low-function value points is higher than the volume occupied by points with high-function value, and hence, can be considered as more diverse. While this implies that sorting can serve as a good heuristic for constructing trajectories transitioning from exploration to exploitation, it does not provide any guidance on the rate for such transitions. Next, we discuss a sampling strategy for explicitly controlling this rate.

Sampling Strategies for Offline Points So far, we have proposed a simple heuristic for transitioning a set of offline points into an explore-then-exploit trajectory. To obtain these offline trajectory points from the offline dataset, one default strategy is to sample uniformly at random T points from \mathcal{D} and sort them. However, we found this strategy to not work well in practice. As Proposition 1 shows, we expect a large volume of the search space to consist of points with low-function values.

Thus, if our offline dataset is uniformly distributed across the domain, the probability of getting a high quality point will be very low with a uniform sampling strategy. To counter this challenge, we propose a 2 step sampling strategy based on binning followed by importance reweighting. Our formulation is motivated by a similar strategy proposed by Kumar and Levine [9] for loss reweighting. First, we use the function values to partition the offline dataset \mathcal{D} into N_B bins of equal-width, i.e., each bin covers a range of equal length. Next, for each bin, we assign a different sampling probability, such that (a) bins where the average function value is high are more likely to be sampled, and (b) bins with more points are sampled more often. The former helps minimize the explore-exploit budget, whereas the latter ensures diversity in trajectories. Based on these two criteria, the score s_i for a bin B_i is given as:

$$s_i = \frac{|B_i|}{|B_i| + K} \exp\left(\frac{-|\hat{y} - y_{b_i}|}{\tau}\right)$$

where \hat{y} is the best function value in the dataset \mathcal{D} , and y_{b_i} is the midpoint of the interval corresponding to the bin B_i . Here, the first term $\frac{|B_i|}{|B_i|+K}$ allows us to assign higher weight to the larger bins with smoothing. The second term gives higher weight to "good" (low regret) bins using an exponential weighting scheme. More details about K and τ can be found in Appendix B. Finally, we use these scores s_i to proportionally sample n_i points from bin B_i where $n_i = T \left[\frac{s_i}{\sum_j s_j} \right]$ for $i \in \{2, \dots, N_B\}$ and $n_1 = T - \sum_{i>1} n_i$, making the overall length of the trajectories equal to T . In Figure 4, we illustrate the shift in distribution of function values due to our sampling strategy. We refer to the combined strategy of sampling and then sorting as SORT-SAMPLE in Figure 3 and Algorithm 1.

Augmenting Trajectories With Regret Budgets Our sorted trajectories reflect roll-outs of implicit black-box optimizers transitioning from exploration to exploitation. However they do not provide us with information on the rate at which a trajectory approaches the optimal value. This information is important as it can help distinguish different trajectories as well as the exploration and exploitation phase within a trajectory. A natural choice for such a knob would be the cumulative regret. Intuitively, a sequence of points with a low cumulative regret reflects more exploitation compared to a sequence with high cumulative regret. Moreover, as we shall show later, cumulative regret provides BOOMER a simple and effective knob to generalize outside the offline dataset during the evaluation phase.

Hence, we propose to augment each data point \mathbf{x}_i in our trajectory with a Regret Budget (RB). The RB R_i at timestep i defined as the cumulative regret of the trajectory, starting at point \mathbf{x}_i : $R_i = \sum_{j=i}^T (f(\mathbf{x}^*) - f(\mathbf{x}_j))$. Intuitively, a high (low) value for R_i is likely to result in a high (low) budget for exploration. Note, we are only assuming knowledge of an estimate for $f(\mathbf{x}^*)$ (and not \mathbf{x}^*). Hence, each trajectory in our desired set $\mathcal{D}_{\text{traj}}$ can be represented as:

$$\mathcal{T} = (R_1, \mathbf{x}_1, R_2, \mathbf{x}_2, \dots, R_T, \mathbf{x}_T) \quad (3)$$

We will refer to R_1 as Initial Regret Budget (IRB) henceforth. This will be of significance for evaluating our model in Phase 3 (Section 2.4), as we can specify a low IRB to force the model to output points close to the optima, or in other words, exploit.

2.3 Phase 2: Training an Autoregressive Generative Model

Given our trajectory dataset, we design our BBO agent as a conditional autoregressive model and train it to maximize the likelihood of trajectories in $\mathcal{D}_{\text{traj}}$. More formally, we denote our model parameterized by θ as $g_\theta(\mathbf{x}_t | \mathbf{x}_{<t}, R_{\leq t})$, where by $k_{<t}$ for some variable k we mean the set $\{k_1, \dots, k_{t-1}\}$. Here, \mathbf{x}_i are the sequence of points in a trajectory, and R_i refers to the regret budget at timestep i .

Building on recent advances in sequence modeling [15, 2, 1], we instantiate our model with a causally masked transformer and train it to maximize the likelihood of our trajectory dataset $\mathcal{D}_{\text{traj}}$.

$$\mathcal{L}(\theta; \mathcal{D}_{\text{traj}}) = \mathbb{E}_{\mathcal{T} \sim \mathcal{D}_{\text{traj}}} \left[\sum_{i=1}^T \log g_\theta(\mathbf{x}_i | \mathbf{x}_{<i}, R_{\leq i}) \right] \quad (4)$$

In practice, we translate this loss to the mean squared error loss for a continuous \mathcal{X} (equivalent to a Gaussian g_θ with fixed variance), and cross entropy loss for a discrete \mathcal{X} .

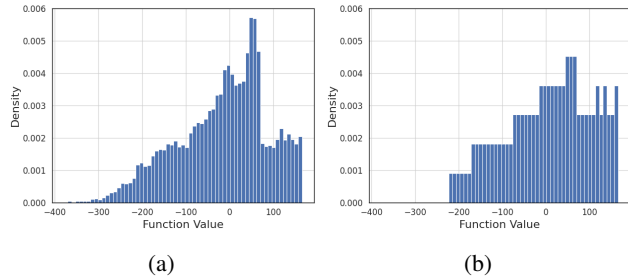


Figure 4: Plots showing the distribution of the function values in the offline dataset \mathcal{D} (left) and the trajectories in $\mathcal{D}_{\text{traj}}$ (right) for the Ant Morphology benchmark [3]. Notice how the overall density of points with high function values is up-weighted post our re-weighting.

2.4 Phase 3: Evaluation Rollout of Final Candidates

Once trained, we can use our BBO agent to directly output new points as its candidate guesses for maximizing the black-box function. We do so by rolling out evaluation trajectories from our model. Each trajectory will be subdivided into a *prefix subsequence* and a *prediction subsequence*. The prefix subsequence consists of $P < T$ points sampled using SORT-SAMPLE from our offline dataset \mathcal{D} as before. These prefix points emphasize the exploration phase of the evaluation trajectory. Thereafter, we rollout the prediction subsequence consisting of $T - P$ points by sampling from our autoregressive generative model.

Setting Regret Budgets One key question relates to setting the regret budget at the start of the suffix subsequence. It is not preferable to set it to R_{P+1} of the sampled trajectory, as doing so will lead to a slow exploitation rate similar to the one observed in the training trajectories. Since the training trajectories do not generalize, this will not allow the the suffix to generalize beyond the offline dataset.

Alternatively, we initialize it to a low value in BOOMER to accelerate the exploitation following a prefix subsequence. We refer to this low value as Evaluation RB and denote it as \hat{R} in Figure 3 and Section 3. Thereafter, we keep the RB for the suffix subsequence fixed (\hat{R}), as the agent is already in the exploitation phase. We choose not to update the evaluation RB since updating here would require sequential querying to the function f , which can be prohibitive. Thus, our evaluation protocol can generate a set of candidate queries purely in an offline manner. In practice, we also find it useful to split the Q candidate points among a few (>1) small \hat{R} values, each with a different prefix length.

3 Experimental Evaluation

We first empirically evaluate BOOMER for optimizing a synthetic 2D function, Branin, in order to analyze its working and probe the various components. Next, we perform large-scale benchmarking and experiments on Design-Bench [3], a suite of offline BBO tasks based on real world problems.

3.1 Branin Task

Branin is a well-known benchmark function for evaluating optimization methods. It is a 2D function evaluated on the ranges $x_1 \in [-5, 10]$ and $x_2 \in [0, 15]$:

$$f_{br}(x_1, x_2) = a(x_2 - bx_1^2 + cx_1 - r)^2 + s(1 - t) \cos x_1 + s \quad (5)$$

where $a = -1$, $b = \frac{5.1}{4\pi^2}$, $c = \frac{5}{\pi}$, $r = 6$, $s = -10$, and $t = \frac{1}{5\pi}$. In this square region, f_{br} has three global maximas, $(-\pi, 12.275)$, $(\pi, 2.275)$, and $(9.42478, 2.475)$; with the maximum value of -0.397887 . Figure 2 shows an illustration of the function contours.

For offline optimization we uniformly sample $N = 5000$ points in the domain, and remove the top 10%-ile (according to the function value) from this set to remove points close to the optima to make the task more challenging. We then construct 400 trajectories of length 64 each according to the SORT-SAMPLE strategy.

During the evaluation, we initialize four trajectories with a prefix length of 32 and unroll them for an additional 32 steps, and output the best result, thus consuming a query budget of 128. As shown in Table 1, BOOMER successfully generalizes beyond the best point in our offline dataset. We also report numbers for a gradient ascent baseline, which uses the offline dataset to train a forward model (a 2 layer NN) mapping \mathbf{x} to y and then performs gradient ascent on \mathbf{x} to infer its optima. Next, we perform ablations to understand the effect of the Evaluation RB \hat{R} and prefix length P on our rolled-out trajectories.

Optima	\mathcal{D} (best)	BOOMER	Grad. Ascent
-0.398	-6.119	-1.79 ± 0.843	-3.953 ± 4.258

Table 1: Best function value achieved by each method on the Branin task. \mathcal{D} (best) refers to the best (lowest regret) value present in the offline dataset \mathcal{D} . We report mean and standard deviation averaged over 5 runs. Gradient ascent performs poorly because on many initialization points, the trajectories escape out of the square domain.

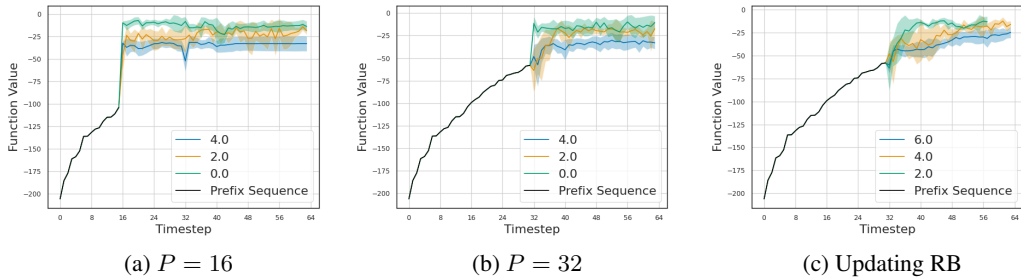


Figure 5: Rolled-out trajectories for Branin task for multiple \hat{R} values (averaged over 5 runs). Figure (b) shows trajectories with prefix length 32, without updating RB (default evaluation setting). In Figure (a), we change the prefix length to 16 while in Figure (c), we update the evaluation RB in the suffix subsequence.

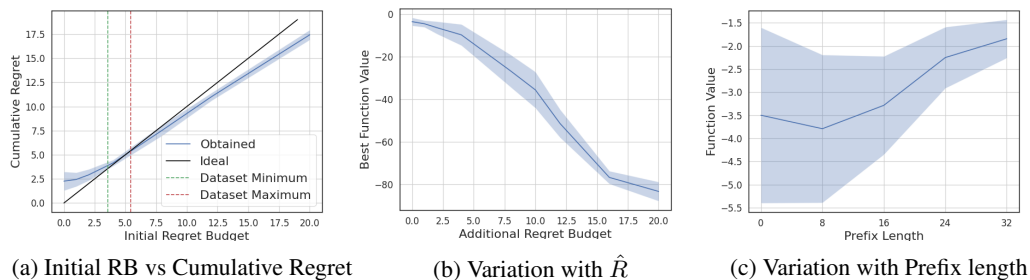


Figure 6: Ablation studies for Branin task. All the values are averaged over 5 runs.

Impact of \hat{R} Figures 5a and 5b shows rolled-out trajectories for our model for different \hat{R} values, with prefix lengths 16 and 32. We see that low \hat{R} rolls out higher quality points compared to high \hat{R} . To verify our semantics of regret budget as a knob for controlling the extent of exploration and exploitation, in the Figure 5c, we also plot trajectories where we update the RB values in the suffix. We stop the roll-out if RB becomes non-positive. It is evident that for smaller \hat{R} , the agent quickly accelerates to high quality regions and keeps exploiting, whereas for high \hat{R} , it gradually shifts to high quality points. This shows how \hat{R} controls the rate of transition from exploration to exploitation.

To further check whether our model has learnt to generate a sequence having cumulative regret close to the initial RB R_1 , we plot R_1 vs the cumulative regret of a full rolled-out sequence in Figure 6a. We observe that the curve is close to the desired ideal line $y = x$. Notice that the range of R_1 values of $\mathcal{D}_{\text{traj}}$ is quite narrow, but BOOMER is able to generalize well to a much wider range, allowing it to propose points even better than the dataset. During training, model has only seen low RB values towards the end of the trajectories. However, the powerful "stitching" ability [16] of the model allows it to roll-out a novel trajectory having low cumulative regret when conditioned on low unseen R_1 values. Finally, since in BBO our goal is to find the best point, we also plot the best rolled-out point across a trajectory vs \hat{R} in the Figure 6b, while keeping the prefix sequence fixed. As expected, we observe a decreasing trend, justifying our choice of small \hat{R} values during evaluation.

Impact of Prefix Length Figure 6c shows the obtained best function values for different prefix lengths, averaged over multiple \hat{R} values, with same query budget $Q = 32$. As expected, we see an increasing trend in the best function value. We also observe a decreasing variance, indicating that the trajectory roll-outs are more stable when augmented with history of points. Note that prefix lengths larger than 32 doesn't perform very well in practice because they have fewer than 32 shots to propose a good point in a single trajectory. Empirically, we found prefix length equal to half of the trajectory length to perform well across the experiments. We provide more details about the ablations, experimental setup, and model hyper-parameters in the Appendix B and C.

Baseline	TFBind8	TFBind10	Superconductor	Ant	D’Kitty	ChEMBL	NAS	Mean Score (↑)	Mean Rank (↓)
\mathcal{D} (best)	0.439	0.467	0.399	0.565	0.884	0.605	0.436	-	-
CbAS	0.958 ± 0.018	0.657 ± 0.017	0.45 ± 0.083	0.876 ± 0.015	0.896 ± 0.016	0.640 ± 0.005	0.683 ± 0.079	0.737 ± 0.033	5.4
BO-qEI	0.824 ± 0.086	0.635 ± 0.011	0.501 ± 0.021	0.887 ± 0.0	0.896 ± 0.0	0.633 ± 0.000	1.009 ± 0.059	0.769 ± 0.026	5.3
CMA-ES	0.933 ± 0.035	0.679 ± 0.034	0.491 ± 0.004	1.436 ± 0.928	0.725 ± 0.002	0.636 ± 0.004	0.985 ± 0.079	0.840 ± 0.156	4.0
Gradient Ascent	0.981 ± 0.015	0.659 ± 0.039	0.504 ± 0.005	0.34 ± 0.034	0.906 ± 0.017	0.647 ± 0.020	0.433 ± 0.000	0.638 ± 0.018	4.0
REINFORCE	0.959 ± 0.013	0.64 ± 0.028	0.481 ± 0.017	0.261 ± 0.042	0.474 ± 0.202	0.636 ± 0.023	-1.895 ± 0.000	0.222 ± 0.046	6.7
MINs	0.938 ± 0.047	0.659 ± 0.044	0.484 ± 0.017	0.942 ± 0.018	0.944 ± 0.009	0.653 ± 0.002	0.717 ± 0.046	0.762 ± 0.026	3.7
COMs	0.964 ± 0.02	0.654 ± 0.02	0.423 ± 0.033	0.949 ± 0.021	0.948 ± 0.006	0.648 ± 0.005	0.459 ± 0.139	0.720 ± 0.034	4.4
BOOMER (Ours)	0.975 ± 0.004	0.681 ± 0.035	0.437 ± 0.022	0.976 ± 0.012	0.954 ± 0.012	0.654 ± 0.019	0.724 ± 0.008	0.772 ± 0.016	2.4

Table 2: Comparative evaluation of BOOMER over 5 tasks averaged over 5 runs. We report normalized scores with $Q = 256$ (except for NAS, where we use $Q = 128$) and highlight the top 2 results in each column. **Blue** denotes the best entry in the column, and **Violet** denotes the second best. We observe that BOOMER is in the top 2 in 5 out of 7 tasks, and is also consistently able to outperform the best offline dataset point in all tasks.

3.2 Design-Bench tasks

Next, we evaluate BOOMER on 5 complex real-world tasks of Design-Bench [3]. These tasks are considered challenging due to high dimensionality, low quality points in the offline dataset, approximate oracles in some cases, and highly sensitive landscapes with narrow optima regions [3].

Discrete The **TFBind8** and **TFBind10** are discrete tasks where the goal is to optimize for a DNA sequence which has maximum affinity to bind with a particular transcription factor. The sequences are of length 8 (10) for TFBind8 (TFBind10), where each element in the sequence is one of 4 bases. The aim in the **ChEMBL** task is to optimize for molecule activity for drug discovery. We make use of an assay with id CHEMBL3885882 and optimize for its MCHC value. The resulting task is 31 dimensional, where each dimension is a categorical variable which can take one of 591 different values. In **NAS**, the goal is to search for a neural network architecture that optimizes for test accuracy in CIFAR10 [17]. The precise architectural choices for this neural network are detailed in [3]. The resulting task is in a 64 dimensional discrete space with 5 categories per dimension.

Continuous In **D’Kitty** and **Ant** morphology tasks, we optimize the morphology of two robots: Ant from OpenAI gym [18] and D’Kitty from ROBEL [19]. In **Superconductor** task, the aim is to find a chemical formula for a superconducting material with high critical temperature. D’Kitty, Ant and Superconductor are continuous tasks with dimensions 56, 60, and 86 respectively. For the first 6 tasks, we have query access to the exact oracle function. For Superconductor, we only have an approximate oracle, which is a random forest regressor trained on a much larger hidden dataset.

Baselines We compare BOOMER with multiple canonical baselines like gradient ascent, REINFORCE [20], BayesOpt [14] and CMA-ES [21]. We also compare with more recent methods like MINs [9], COMs [8] and CbAS [10].²For inherently active methods, instead of performing BayesOpt on the oracle function, we perform BayesOpt on a surrogate model (a feedforward NN) trained on the offline dataset. MINs [9] also train a forward model to optimize over the conditioning parameters. Our method does not need a separate forward model, and thus, is not dependent on the quality of the fit of the forward model.

Evaluation We allow a query budget of $Q = 256$ for all the baselines, except for NAS, where due to lack of compute we make use of $Q = 128$. For BOOMER, across all tasks, we rollout 4 trajectories, each with a prefix and prediction subsequence length of 64 each. The prediction subsequence is initialized with one of 4 candidate low \hat{R} values $\{0, 0.01, 0.05, 0.1\}$ (for NAS we only use $\hat{R} \in \{0, 0.01\}$). For each \hat{R} , we then roll-out for 64 timesteps, and choose the best point. We collect results over 5 trials, and report the mean and standard deviation for each of the models and tasks in Table 2. Following the procedure used by [8, 3, 22], the results of Table 2 are linearly normalized between the minimum and maximum values of a much larger hidden offline dataset.

Results Overall, we obtain a mean score of 0.772 and an average rank of 2.4, which is the best among all the baselines. We achieve best results on two tasks - TF-Bind-10 (discrete) and D’Kitty (continuous). Additionally, we are among top 2 for five out of seven tasks. We show significant

²We take the baseline implementations from <https://github.com/brandontrabucco/design-baselines>

improvements over generative methods such as MINs [9] or CbAS [10], and forward mapping methods such as COMs [8] on TF-Bind-8, TF-Bind-10, Ant and D’Kitty. We also note that while BOOMER is placed second in Ant, it shows a much lower standard deviation (0.012) compared to the to the best performing method CMA-ES, which has a much larger standard deviation of 0.928. We also have a lowest mean standard deviation across all tasks, suggesting that BOOMER is less sensitive to bad initializations compared to other methods. We report the un-normalized results, ablations and other experimental details for Design-Bench tasks in Appendix C.

4 Related Work

Active BBO The majority of prior work in BBO have been in the active setting, where surrogate models are allowed to query the function during training. This includes long bodies of work in Bayesian Optimization, e.g., [14, 23, 24] and bandits, e.g., [13, 25, 26, 27, 28, 29, 30]. Such methods usually employ surrogate models such as Gaussian Processes [24], Neural Processes [31, 32, 33, 34, 35] or Bayesian Neural Networks [36, 37] to approximate the black-box function, and an uncertainty-aware acquisition strategy for querying new points. However, they are usually computationally expensive and can benefit immensely from offline datasets [3].

Offline BBO Recent works have made use of such datasets and shown promising results [9, 8, 10, 11, 38, 39, 22]. Kumar and Levine [9] train a stochastic inverse mapping from the outputs y to inputs x using a generative model similar to a conditional GAN [40, 41, 42, 43]. They then optimize over y to find a good design point. Training GANs however can be difficult due to issues like mode collapse [42]. Other methods make use of gradient ascent to find an optimal solution. Trabucco et al. [8] and Yu et al. [22] train a model to be robust to outliers by regularizing the objective such that they assign low score to those points. Fu and Levine [38] train a normalized maximum likelihood estimate of the function. We instead offer a fresh perspective based on generative sequence modelling and we show strong results in comparison to many of these prior works in Section 3.

Offline reinforcement learning (RL) While both RL and BBO are sequential decision making problems, the key difference is that RL is stateful while BBO is not. In the offline setting [44, 30], both problems require models or policies that can generalize beyond the offline dataset to achieve good performance. Related to our work, autoregressive transformers have been successfully applied on trajectory data obtained from offline RL [16, 45, 46]. However, there are important differences between their setting and offline BBO. For example, the data in offline BBO is not sequential in nature, unlike in offline RL where the offline data is naturally in the form of demonstrations. One of our contributions is to design a notion of ‘explore-then-exploit’ sequences to BBO for autoregressive modeling and test-time generalization.

Transformers The transformer architecture [15] has been used extensively for many natural language [2, 15, 1] and computer vision [47, 48] tasks among other modalities [49], achieving state-of-the-art performance on many domains and benchmarks. Future algorithmic and architectural advancements in these models can therefore directly translate to improvements to BOOMER and in turn, BOOMER can be easily integrated to solving BBO problems with inputs from vision and language modalities.

5 Discussion

We presented BOOMER, a novel generative framework for pretraining black-box optimizers using offline data. BOOMER consists of a 3 phased process. In the first phase, we use a novel SORT-SAMPLE strategy to generate trajectories from offline data that use the sorting heuristic to transition from exploration to exploitation. We further provide a mechanism for controlling the degree of exploration and exploitation via regret budget. In phases 2 and 3, we train our model using an autoregressive transformer and use it to generate candidate points that maximize the black-box function. Experimentally, we verify that BOOMER is capable of solving complex high dimensional tasks like the ones in Design-Bench, achieving an average rank of **2.4** with a mean score of **0.772**.

Limitations and Future Work We are interested in extending BOOMER to an active setting where our model can quantify uncertainty and actively query the black-box function after pretraining on an

offline dataset. On a practical side, we would also be interested in analyzing the properties of domains that dictate where BOOMER can strongly excel (e.g., D’Kitty) or struggle (e.g., Superconductor) relative to other approaches. Finally, we aim to expand our scope to a meta-task setting, where instead of single function, our offline data consists of past evaluation from multiple black-box functions.

Acknowledgments and Disclosure of Funding

We would like to thank Shashak Goel, Hritik Bansal and Tung Nguyen for their valuable feedback on earlier drafts of this paper. This work used computational and storage services associated with the Hoffman2 Shared Cluster provided by UCLA Institute for Digital Research and Education’s Research Technology Group.

References

- [1] Alec Radford, Jeff Wu, Rewon Child, David Luan, Dario Amodei, and Ilya Sutskever. Language models are unsupervised multitask learners. 2019.
- [2] Tom Brown, Benjamin Mann, Nick Ryder, Melanie Subbiah, Jared D Kaplan, Prafulla Dhariwal, Arvind Neelakantan, Pranav Shyam, Girish Sastry, Amanda Askell, Sandhini Agarwal, Ariel Herbert-Voss, Gretchen Krueger, Tom Henighan, Rewon Child, Aditya Ramesh, Daniel Ziegler, Jeffrey Wu, Clemens Winter, Chris Hesse, Mark Chen, Eric Sigler, Mateusz Litwin, Scott Gray, Benjamin Chess, Jack Clark, Christopher Berner, Sam McCandlish, Alec Radford, Ilya Sutskever, and Dario Amodei. Language models are few-shot learners. In *Advances in Neural Information Processing Systems*, 2020.
- [3] Brandon Trabucco, Xinyang Geng, Aviral Kumar, and Sergey Levine. Design-bench: Benchmarks for data-driven offline model-based optimization. *CoRR*, abs/2202.08450, 2022. URL <https://arxiv.org/abs/2202.08450>.
- [4] Jeffrey Larson, Matt Menickelly, and Stefan M. Wild. Derivative-free optimization methods. *Acta Numerica*, 28:287–404, may 2019. doi: 10.1017/s0962492919000060. URL <https://doi.org/10.1017%2Fs0962492919000060>.
- [5] Bobak Shahriari, Kevin Swersky, Ziyu Wang, Ryan P. Adams, and Nando de Freitas. Taking the human out of the loop: A review of bayesian optimization. *Proceedings of the IEEE*, 104(1):148–175, 2016. doi: 10.1109/JPROC.2015.2494218.
- [6] Reuven Y. Rubinstein and Dirk P. Kroese. *The Cross Entropy Method: A Unified Approach To Combinatorial Optimization, Monte-Carlo Simulation (Information Science and Statistics)*. Springer-Verlag, Berlin, Heidelberg, 2004. ISBN 038721240X.
- [7] Peter M Attia, Aditya Grover, Norman Jin, Kristen A Severson, Todor M Markov, Yang-Hung Liao, Michael H Chen, Bryan Cheong, Nicholas Perkins, Zi Yang, et al. Closed-loop optimization of fast-charging protocols for batteries with machine learning. *Nature*, 578(7795): 397–402, 2020.
- [8] Brandon Trabucco, Aviral Kumar, Xinyang Geng, and Sergey Levine. Conservative objective models for effective offline model-based optimization. In Marina Meila and Tong Zhang, editors, *Proceedings of the 38th International Conference on Machine Learning*, volume 139 of *Proceedings of Machine Learning Research*, pages 10358–10368. PMLR, 18–24 Jul 2021. URL <https://proceedings.mlr.press/v139/trabucco21a.html>.
- [9] Aviral Kumar and Sergey Levine. Model inversion networks for model-based optimization. In H. Larochelle, M. Ranzato, R. Hadsell, M.F. Balcan, and H. Lin, editors, *Advances in Neural Information Processing Systems*, volume 33, pages 5126–5137. Curran Associates, Inc., 2020. URL <https://proceedings.neurips.cc/paper/2020/file/373e4c5d8edfa8b74fd4b6791d0cf6dc-Paper.pdf>.
- [10] David Brookes, Hahnbeom Park, and Jennifer Listgarten. Conditioning by adaptive sampling for robust design. In Kamalika Chaudhuri and Ruslan Salakhutdinov, editors, *Proceedings of the 36th International Conference on Machine Learning*, volume 97 of *Proceedings of Machine*

- Learning Research*, pages 773–782. PMLR, 09–15 Jun 2019. URL <https://proceedings.mlr.press/v97/brookes19a.html>.
- [11] Clara Fannjiang and Jennifer Listgarten. Autofocused oracles for model-based design, 2020. URL <https://arxiv.org/abs/2006.08052>.
- [12] Wenshuo Guo, Kumar Krishna Agrawal, Aditya Grover, Vidya Muthukumar, and Ashwin Pananjady. Learning from an exploring demonstrator: Optimal reward estimation for bandits, 2021. URL <https://arxiv.org/abs/2106.14866>.
- [13] Aurélien Garivier, Emilie Kaufmann, and Tor Lattimore. On explore-then-commit strategies. In *Proceedings of the 30th International Conference on Neural Information Processing Systems, NIPS’16*, page 784–792, Red Hook, NY, USA, 2016. Curran Associates Inc. ISBN 9781510838819.
- [14] Jasper Snoek, Hugo Larochelle, and Ryan P. Adams. Practical bayesian optimization of machine learning algorithms, 2012. URL <https://arxiv.org/abs/1206.2944>.
- [15] Ashish Vaswani, Noam Shazeer, Niki Parmar, Jakob Uszkoreit, Llion Jones, Aidan N Gomez, Łukasz Kaiser, and Illia Polosukhin. Attention is all you need. In I. Guyon, U. Von Luxburg, S. Bengio, H. Wallach, R. Fergus, S. Vishwanathan, and R. Garnett, editors, *Advances in Neural Information Processing Systems*, volume 30. Curran Associates, Inc., 2017. URL <https://proceedings.neurips.cc/paper/2017/file/3f5ee243547dee91fbd053c1c4a845aa-Paper.pdf>.
- [16] Lili Chen, Kevin Lu, Aravind Rajeswaran, Kimin Lee, Aditya Grover, Michael Laskin, Pieter Abbeel, Aravind Srinivas, and Igor Mordatch. Decision transformer: Reinforcement learning via sequence modeling. *arXiv preprint arXiv:2106.01345*, 2021.
- [17] Alex Krizhevsky, Vinod Nair, and Geoffrey Hinton. Cifar-10 (canadian institute for advanced research). URL <http://www.cs.toronto.edu/~kriz/cifar.html>.
- [18] Greg Brockman, Vicki Cheung, Ludwig Pettersson, Jonas Schneider, John Schulman, Jie Tang, and Wojciech Zaremba. Openai gym, 2016.
- [19] Michael Ahn, Henry Zhu, Kristian Hartikainen, Hugo Ponte, Abhishek Gupta, Sergey Levine, and Vikash Kumar. Robel: Robotics benchmarks for learning with low-cost robots. 2019. doi: 10.48550/ARXIV.1909.11639. URL <https://arxiv.org/abs/1909.11639>.
- [20] Richard S Sutton, David McAllester, Satinder Singh, and Yishay Mansour. Policy gradient methods for reinforcement learning with function approximation. In S. Solla, T. Leen, and K. Müller, editors, *Advances in Neural Information Processing Systems*, volume 12. MIT Press, 1999. URL <https://proceedings.neurips.cc/paper/1999/file/464d828b85b0bed98e80ade0a5c43b0f-Paper.pdf>.
- [21] Nikolaus Hansen. *The CMA Evolution Strategy: A Comparing Review*, pages 75–102. Springer Berlin Heidelberg, Berlin, Heidelberg, 2006. ISBN 978-3-540-32494-2. doi: 10.1007/3-540-32494-1_4. URL https://doi.org/10.1007/3-540-32494-1_4.
- [22] Sihyun Yu, Sungsoo Ahn, Le Song, and Jinwoo Shin. RoMA: Robust model adaptation for offline model-based optimization. In A. Beygelzimer, Y. Dauphin, P. Liang, and J. Wortman Vaughan, editors, *Advances in Neural Information Processing Systems*, 2021. URL <https://openreview.net/forum?id=VH0TRmnqUc>.
- [23] Kevin Swersky, Jasper Snoek, and Ryan P Adams. Multi-task bayesian optimization. In C.J. Burges, L. Bottou, M. Welling, Z. Ghahramani, and K.Q. Weinberger, editors, *Advances in Neural Information Processing Systems*, volume 26. Curran Associates, Inc., 2013. URL <https://proceedings.neurips.cc/paper/2013/file/f33ba15effa5c10e873bf3842afb46a6-Paper.pdf>.
- [24] Niranjan Srinivas, Andreas Krause, Sham Kakade, and Matthias W. Seeger. Gaussian Process Optimization in the Bandit Setting: No Regret and Experimental Design. In *Proceedings of the 27th International Conference on Machine Learning*, pages 1015–1022. Omnipress, 2010.

- [25] Carlos Riquelme, George Tucker, and Jasper Snoek. Deep bayesian bandits showdown: An empirical comparison of bayesian deep networks for thompson sampling. *arXiv preprint arXiv:1802.09127*, 2018.
- [26] Thorsten Joachims, Adith Swaminathan, and Maarten de Rijke. Deep learning with logged bandit feedback. In *International Conference on Learning Representations*, 2018. URL https://openreview.net/forum?id=SJaP_-xAb.
- [27] Aditya Grover, Todor Markov, Peter Attia, Norman Jin, Nicholas Perkins, Bryan Cheong, Michael Chen, Zi Yang, Stephen Harris, William Chueh, and Stefano Ermon. Best arm identification in multi-armed bandits with delayed feedback. In *International Conference on Artificial Intelligence and Statistics (AISTATS)*, 2018.
- [28] T. Joachims, A. Swaminathan, and M. de Rijke. Deep learning with logged bandit feedback. In *International Conference on Learning Representations (ICLR)*, 2018.
- [29] Adith Swaminathan and Thorsten Joachims. Batch learning from logged bandit feedback through counterfactual risk minimization. *Journal of Machine Learning Research*, 16(52): 1731–1755, 2015. URL <http://jmlr.org/papers/v16/swaminathan15a.html>.
- [30] Alexis Jacq, Matthieu Geist, Ana Paiva, and Olivier Pietquin. Learning from a learner. In Kamalika Chaudhuri and Ruslan Salakhutdinov, editors, *Proceedings of the 36th International Conference on Machine Learning*, volume 97 of *Proceedings of Machine Learning Research*, pages 2990–2999. PMLR, 09–15 Jun 2019. URL <https://proceedings.mlr.press/v97/jacq19a.html>.
- [31] Marta Garnelo, Dan Rosenbaum, Christopher Maddison, Tiago Ramalho, David Saxton, Murray Shanahan, Yee Whye Teh, Danilo Rezende, and S. M. Ali Eslami. Conditional neural processes. In Jennifer Dy and Andreas Krause, editors, *Proceedings of the 35th International Conference on Machine Learning*, volume 80 of *Proceedings of Machine Learning Research*, pages 1704–1713. PMLR, 10–15 Jul 2018. URL <https://proceedings.mlr.press/v80/garnelo18a.html>.
- [32] Marta Garnelo, Jonathan Schwarz, Dan Rosenbaum, Fabio Viola, Danilo J Rezende, SM Eslami, and Yee Whye Teh. Neural processes. *arXiv preprint arXiv:1807.01622*, 2018.
- [33] Jonathan Gordon, Wessel P Bruinsma, Andrew YK Foong, James Requeima, Yann Dubois, and Richard E Turner. Convolutional conditional neural processes. *arXiv preprint arXiv:1910.13556*, 2019.
- [34] Anonymous. Neural bootstrapping attention for neural processes. In *Submitted to The Tenth International Conference on Learning Representations*, 2022. URL <https://openreview.net/forum?id=Z7VhFVRVqeU>. under review.
- [35] Gautam Singh, Jaesik Yoon, Youngsung Son, and Sungjin Ahn. Sequential neural processes. *arXiv preprint arXiv:1906.10264*, 2019.
- [36] Daniel T. Chang. Bayesian neural networks: Essentials, 2021. URL <https://arxiv.org/abs/2106.13594>.
- [37] Ethan Goan and Clinton Fookes. Bayesian neural networks: An introduction and survey. In *Case Studies in Applied Bayesian Data Science*, pages 45–87. Springer International Publishing, 2020. doi: 10.1007/978-3-030-42553-1_3. URL https://doi.org/10.1007/978-3-030-42553-1_3.
- [38] Justin Fu and Sergey Levine. Offline model-based optimization via normalized maximum likelihood estimation. In *International Conference on Learning Representations*, 2021. URL <https://openreview.net/forum?id=FmMKS04e8JK>.
- [39] Kourosh Hakhamaneshi, Pieter Abbeel, Vladimir Stojanovic, and Aditya Grover. Jumbo: Scalable multi-task bayesian optimization using offline data. *arXiv preprint arXiv:2106.00942*, 2021.

- [40] Ian Goodfellow, Jean Pouget-Abadie, Mehdi Mirza, Bing Xu, David Warde-Farley, Sherjil Ozair, Aaron Courville, and Yoshua Bengio. Generative adversarial nets. In Z. Ghahramani, M. Welling, C. Cortes, N. Lawrence, and K.Q. Weinberger, editors, *Advances in Neural Information Processing Systems*, volume 27. Curran Associates, Inc., 2014. URL <https://proceedings.neurips.cc/paper/2014/file/5ca3e9b122f61f8f06494c97b1afccf3-Paper.pdf>.
- [41] Mehdi Mirza and Simon Osindero. Conditional generative adversarial nets, 2014. URL <https://arxiv.org/abs/1411.1784>.
- [42] Martin Arjovsky, Soumith Chintala, and Léon Bottou. Wasserstein generative adversarial networks. In Doina Precup and Yee Whye Teh, editors, *Proceedings of the 34th International Conference on Machine Learning*, volume 70 of *Proceedings of Machine Learning Research*, pages 214–223. PMLR, 06–11 Aug 2017. URL <https://proceedings.mlr.press/v70/arjovsky17a.html>.
- [43] Sebastian Nowozin, Botond Cseke, and Ryota Tomioka. f-gan: Training generative neural samplers using variational divergence minimization. In D. Lee, M. Sugiyama, U. Luxburg, I. Guyon, and R. Garnett, editors, *Advances in Neural Information Processing Systems*, volume 29. Curran Associates, Inc., 2016. URL <https://proceedings.neurips.cc/paper/2016/file/cedebb6e872f539bef8c3f919874e9d7-Paper.pdf>.
- [44] Juergen Schmidhuber. Reinforcement learning upside down: Don’t predict rewards – just map them to actions, 2019. URL <https://arxiv.org/abs/1912.02875>.
- [45] Michael Janner, Qiyang Li, and Sergey Levine. Offline reinforcement learning as one big sequence modeling problem. In *Advances in Neural Information Processing Systems*, 2021.
- [46] Qinqing Zheng, Amy Zhang, and Aditya Grover. Online decision transformer. *arXiv preprint arXiv:2202.05607*, 2022.
- [47] Alexey Dosovitskiy, Lucas Beyer, Alexander Kolesnikov, Dirk Weissenborn, Xiaohua Zhai, Thomas Unterthiner, Mostafa Dehghani, Matthias Minderer, Georg Heigold, Sylvain Gelly, Jakob Uszkoreit, and Neil Houlsby. An image is worth 16x16 words: Transformers for image recognition at scale. In *International Conference on Learning Representations*, 2021. URL <https://openreview.net/forum?id=YicbFdNTTy>.
- [48] Nicolas Carion, Francisco Massa, Gabriel Synnaeve, Nicolas Usunier, Alexander Kirillov, and Sergey Zagoruyko. End-to-end object detection with transformers, 2020. URL <https://arxiv.org/abs/2005.12872>.
- [49] Kevin Lu, Aditya Grover, Pieter Abbeel, and Igor Mordatch. Pretrained transformers as universal computation engines. *arXiv preprint arXiv:2103.05247*, 2021.

A Notations & Proofs

A.1 Notations

Symbol	Meaning
f	Black box function
\mathcal{X}	Support of f
\mathbf{x}^*	Optima (taken to be maxima for consistency)
\mathcal{D}	Offline dataset
N	Size of offline dataset
$\mathcal{D}_{\text{traj}}$	Trajectory dataset
num_traj	Number of trajectories in $\mathcal{D}_{\text{traj}}$
\mathcal{T}	A trajectory
T	Length of a trajectory
Q	Query budget for black-box function
P	Prefix length
R_i	Regret Budget at timestep i
\hat{R}_1	Initial Regret Budget
\hat{R}	Evaluation Regret Budget
g_θ	Autoregressive generative model with parameters θ
K, τ	SORT-SAMPLE hyperparameters
N_B	Number of bins
C	Context Length

Table 3: Important notations used in the paper

A.2 Proofs

Proposition 1 Let $f : [a, b] \rightarrow \mathbb{R}$, $a, b \in \mathbb{R}$, be a real-valued, continuous and differentiable function such that the $f(a)$ and $f(b)$ are not ϵ -high. Let $H \subseteq [a, b]$ be a Lebesgue-measurable set of x values for which $f(x)$ is ϵ -high, with $\epsilon > 0.5$. Let $H^c = [a, b] \setminus H$. Without loss of generality, let's assume that $f(a) \leq f(b)$. If the Lipchitz constant L of f is upper bounded by

$$\frac{2(\epsilon(y_{max} - y_{min}) + y_{min} - f(a))}{b - a}, \quad (6)$$

then $|H| < |H^c|$, where $|\cdot|$ denotes volume of a set w.r.t. the Lebesgue Measure.

Proof of Proposition 1.

Note that if no point in the domain $[a, b]$ achieves ϵ -high function value, then the statement holds trivially true. So, we assume that there is atleast one point which has ϵ -high function value. Let x_1 and x_2 be the smallest and largest such points in the domain. Since the boundary points doesn't have ϵ -high values, $|H^c| \geq (x_1 - a) + (b - x_2)$ and $|H| \leq (x_2 - x_1)$. Thus, if we prove that $(x_1 - a) + (b - x_2) \geq (x_2 - x_1)$, then we are done. To prove this, we try to prove $(x_1 - a) \geq (x_2 - x_1)$.

Assume, on the contrary, that $(x_1 - a) < (x_2 - x_1)$. Rearranging, we get

$$\frac{2}{x_2 - a} < \frac{1}{x_1 - a} \quad (7)$$

Now, by the definition of Lipchitz constant, we have:

$$\begin{aligned} \frac{f(x_1) - f(a)}{x_1 - a} &\leq L \\ \Rightarrow \frac{2(f(x_1) - f(a))}{x_2 - a} &\stackrel{\tau}{\leq} L \\ \Rightarrow \frac{2(\epsilon * (y_{max} - y_{min}) + y_{min} - f(a))}{b - a} &\leq L \end{aligned} \quad (8)$$

Last inequality holds because $x_2 - a \leq b - a$. This inequality contradicts the bound 6 on L , completing our proof for Proposition 1. \square

Now, we show an extension of this proposition for D -dimensional functions with hypercube domains.

Proposition 2. *Let $f : \mathcal{X} \rightarrow \mathbb{R}$ be a D -dimensional, real-valued, continuous, and differentiable function with hypercube domain $\mathcal{X} = [a_1, b_1] \times [a_2, b_2], \dots, \times [a_D, b_D]$, such that none of the boundary points are ϵ -high, for some fixed ϵ . Here by boundary points we mean the points on the surface of the domain hypercube. Let y_{max} and y_{min} be the maximum and the minimum values attained by f . Let $H \subseteq \mathcal{X}$ be a Lebesgue-measurable set of points for which $f(\mathbf{x})$ is ϵ -high. Let $H^c = \mathcal{X} \setminus H$. If the Lipchitz constant L of f is upper bounded by*

$$\frac{2(\epsilon * (y_{max} - y_{min}) + y_{min} - \max_{x_2, \dots, x_D} f(a_1, x_2, \dots, x_D))}{b_1 - a_1}, \quad (9)$$

then $|H| < |H^c|$, where $|\cdot|$ denotes volume of a set w.r.t. the Lebesgue Measure.

Proof. We prove this proposition by induction on the number of dimensions D . Notice that for $D = 1$, the statement reduces to Proposition 1, which we have already proved. Next, we assume that the statement holds for $(D - 1)$ -dimensional functions and prove it for D dimensions, with $D > 1$.

Let's define $\mathcal{H}_{D,\epsilon} : \mathcal{F}_D \rightarrow \mathcal{B}_D$ to be a functional that maps any D -dimensional function, say f , to a Lebesgue-measurable subset of \mathbb{R}^D that corresponds to the set of points where $f(\mathbf{x})$ is ϵ -high. Here, \mathcal{F}_D and \mathcal{B}_D denote the set of all D -dimensional functions and the set of all Lebesgue-measurable subsets of \mathbb{R}^D respectively.

We similarly define the mapping $\mathcal{H}_{D,\epsilon}^c$ to be a functional mapping a function f to the complement of its ϵ -high region. Thus, $H = \mathcal{H}_{D,\epsilon}(f)$ and $H^c = \mathcal{H}_{D,\epsilon}^c(f)$. Now, by definition,

$$|\mathcal{H}_{D,\epsilon}(f(\cdot, \dots, \cdot))| = \int_{x_D} |\mathcal{H}_{D-1,\epsilon}(f(\cdot, \dots, \cdot, x_D))| dx_D \quad (10)$$

And similarly,

$$|\mathcal{H}_{D,\epsilon}^c(f(\cdot, \dots, \cdot))| = \int_{x_D} |\mathcal{H}_{D-1,\epsilon}^c(f(\cdot, \dots, \cdot, x_D))| dx_D \quad (11)$$

Consequently, to prove $|\mathcal{H}_{D,\epsilon}(f(\cdot, \dots, \cdot))| \leq |\mathcal{H}_{D,\epsilon}^c(f(\cdot, \dots, \cdot))|$, we prove $|\mathcal{H}_{D-1,\epsilon}(f(\cdot, \dots, \cdot, x_D))| \leq |\mathcal{H}_{D-1,\epsilon}^c(f(\cdot, \dots, \cdot, x_D))|$ for every $x_D \in [a_D, b_D]$.

To do this, we first fix the D^{th} dimension to be c . In other words, we are considering the $(D - 1)$ -dimensional slice of $f(x_1, \dots, x_D)$ with $x_D = c$. Let g be such a slice with $g(x_1, \dots, x_{D-1}) = f(x_1, \dots, x_{D-1}, c)$. First we need ϵ^g for which ϵ^g -high value for g is ϵ -high for f :

$$\epsilon^g (y_{max}^g - y_{min}^g) + y_{min}^g = \epsilon (y_{max} - y_{min}) + y_{min} \quad (12)$$

where y_{max}^g and y_{min}^g are the minimum and maximum values respectively achieved by g . By this choice of ϵ^g , we are ensuring that a point (x_1, \dots, x_{D-1}, c) is ϵ -high w.r.t f if and only if (x_1, \dots, x_{D-1}) is ϵ^g -high w.r.t g . In other words,

$$\begin{aligned} \mathcal{H}_{D-1,\epsilon^g}(g) &= \mathcal{H}_{D-1,\epsilon}(f(\cdot, \dots, \cdot, c)) \\ \mathcal{H}_{D-1,\epsilon^g}^c(g) &= \mathcal{H}_{D-1,\epsilon}^c(f(\cdot, \dots, \cdot, c)) \end{aligned} \quad (13)$$

Let the Lipchitz constant of g be L^g . First we show that $L_g \leq L$. By definition of Lipchitz constant, for $\mathbf{x} = (x_1, \dots, x_{D-1})$, $\mathbf{z} = (z_1, \dots, z_{D-1})$ in the domain of g ,

$$\begin{aligned} L_g &= \sup_{\mathbf{x} \neq \mathbf{z}} \frac{|g(x_1, \dots, x_{D-1}) - g(z_1, \dots, z_{D-1})|}{\sqrt{\sum_{i=1}^{D-1} (x_i - z_i)^2}} \\ &= \sup_{\mathbf{x} \neq \mathbf{z}} \frac{|f(x_1, \dots, x_{D-1}, c) - f(z_1, \dots, z_{D-1}, c)|}{\sqrt{\sum_{i=1}^{D-1} (x_i - z_i)^2 + (c - c)^2}} \\ &\leq L \end{aligned} \quad (14)$$

Where last inequality is by definition of L w.r.t f . Combining this with our bound on L in 9, we get

$$\begin{aligned}
 L_g &\leq \frac{2(\epsilon * (y_{max} - y_{min}) + y_{min} - \max_{x_2, \dots, x_D} f(a_1, x_2, \dots, x_D))}{b_1 - a_1} \\
 &\leq \frac{2(\epsilon * (y_{max} - y_{min}) + y_{min} - \max_{x_2, \dots, x_{D-1}} f(a_1, x_2, \dots, c))}{b_1 - a_1} \quad (\text{fixing } D^{th} \text{ dimension}) \quad (15) \\
 &\stackrel{12}{\leq} \frac{2(\epsilon^g * (y_{max}^g - y_{min}^g) + y_{min}^g - \max_{x_2, \dots, x_{D-1}} g(a_1, x_2, \dots, x_{D-1}))}{b_1 - a_1}
 \end{aligned}$$

Thus, the Lipchitz bound assumption is followed by g with $\epsilon = \epsilon^g$. Also, the boundaries are not ϵ^g -high w.r.t g because of the choice of ϵ^g . This implies, by inductive assumption, that $|\mathcal{H}_{D-1, \epsilon^g}(g)| \leq |\mathcal{H}_{D-1, \epsilon^g}^c(g)|$. This, combined with equality 13 proves that that $|\mathcal{H}_{D-1, \epsilon}(f(\cdot, \dots, \cdot, c))| \leq |\mathcal{H}_{D-1, \epsilon}^c(f(\cdot, \dots, \cdot, c))|$. Since this is true for all $c \in [a_D, b_D]$, by equations 10 and 11, our proof for $|\mathcal{H}_{D, \epsilon}(f(\cdot, \dots, \cdot))| \leq |\mathcal{H}_{D, \epsilon}^c(f(\cdot, \dots, \cdot))|$ is complete. \square

B Experimental Details

B.1 SORT-SAMPLE

In SORT-SAMPLE, the score of each bin is calculated according to the formula

$$s_i = \frac{|B_i|}{|B_i| + K} \exp\left(\frac{-|\hat{y} - y_{b_i}|}{\tau}\right)$$

The two variables K and τ here act as smoothing parameters. K controls the relative priority given to the larger bins (bins with more points). Higher value of K assigns higher relative weight to these large bins compared to smaller bins, whereas a low value of K the weight assigned to large and small bins would be similar. In the extreme case where $K = 0$, the weight due to $\frac{|B_i|}{|B_i| + K}$ will always be 1, regardless of bin size. For very large value of K , the weight will be approximately linearly proportional to the bin size $|B_i|$. The later case is not desirable because if there is a bin which has very large number of points (which might be a low quality bin), then most of the total weight will be given to that bin because of the linear proportionality.

Temperature τ controls how harshly the bad bins are penalized. Lower the τ value, lower the relative score of the low quality bins (bins with high regret) and vice versa.

In our experiments, we don't tune the values of K , τ , and number of bins N_B . In all the tasks, we use $K = 0.03 \times N$ and $\tau = R_{10}$, where R_{10} is the 10th percentile regret value in \mathcal{D} . For Branin task, we use, $N_B = 32$ and for all the Design-Bench tasks, we use $N_B = 64$. Empirically, as we show in Figure 7a, we didn't observe much effect on K in the range $[0.01, 0.1]$, and for τ from the 50th to the 10th percentiles of R . Figure 7b shows variation with N_B , keeping all other parameters fixed. As expected, $N_B = 1$ doesn't perform well, as having just one bin is equivalent to having no re-weighting. Beyond 32, we don't see much variation with the value of N_B .

B.2 Model architecture & implementation

Architecture We use a GPT [1] like architecture, where each timestep refers to two tokens R_t and \mathbf{x}_t . Similar to Chen et al. [16], we add a new learned timestep embedding (in addition to the positional embedding already present in transformers). Each token R_t and \mathbf{x}_t that goes as input to our model is first projected into a 128 dimensional embedding space using a linear embedding layer. To this embedding, we also add the positional and timestep embeddings. This is passed through a vanilla causally masked transformer. The prediction head for R_t predicts $\hat{\mathbf{x}}_t$, which is then used to compute the loss. The output of the prediction head for \mathbf{x}_t is discarded. At each timestep, we feed in the last C timesteps to the model, where C here refers to the context length. For continuous tasks, the prediction head for R_t outputs a d -dimensional prediction $\hat{\mathbf{x}}_t$. For discrete tasks, the prediction head outputs a $V \times d$ -dimensional prediction, where V refers to the number of classes in the discrete task. Thus, each dimension in \mathcal{X} corresponds to a V -dimensional logits vector.

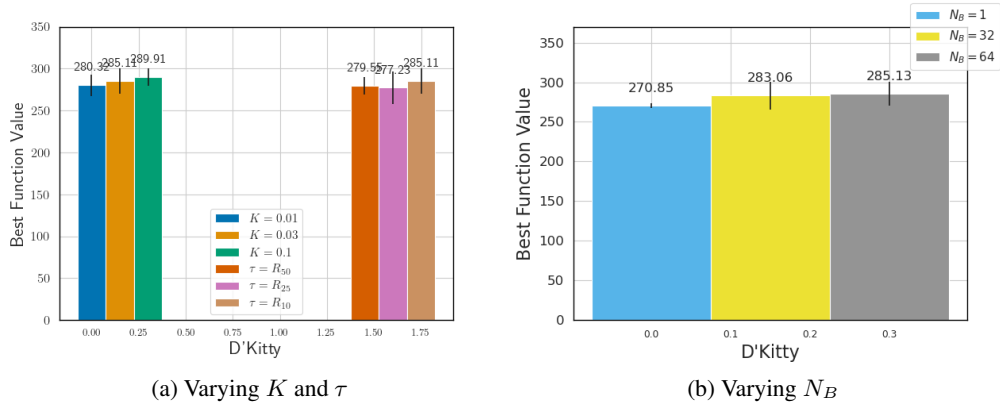


Figure 7: We plot the best achieved function value for different combinations of K , τ and N_B . As expected, we don't see much sensitivity to the choice of K and τ . For N_B , as expected, we a significant decrease for $N_B = 1$, but $N_B = 32$ is comparable to $N_B = 64$

Code Our code (available at the anonymized link here) is built upon the code from minGPT³ and Chen et al. [16]⁴. All code we use is under the MIT licence.

Training The parameter details for all the tasks are summarized in the Table 4. Note that almost all of the parameters are same across all the Design-Bench tasks. Number of layers is higher for continuous tasks, as they are of higher dimensionalities. For all the tasks, we use a batch size of 128 and a fixed learning rate of 10^{-4} for 75 epochs. All training is done using 10 Intel(R) Xeon(R) CPU cores (E5-2698 v4443 @ 2.20GHz) and one NVIDIA Tesla V100 SXM2 GPU.

B.3 Evaluation

For all the Design-Bench tasks, we use a query budget $Q = 256$. Since we use a trajectory length of 128 and a prefix length of 64, this means that we can roll-out four different trajectories. There are two variable parameters during the evaluation: Evaluation RB (\hat{R}) and the prefix sub-sequence. We empirically observed that \hat{R} has more impact on the variability of rolled-out points compared to prefix sub-sequence. Hence, we roll-out trajectory for 4 different low \hat{R} values (0.0, 0.01, 0.05, 0.1). These values are kept fixed across all the tasks and are not tuned. They are chosen to probe the interval $[0.0, 0.1]$, while giving slightly more importance to the low values by choosing 0.01. Evaluation strategies with lower query budget Q available are discussed in the section C.2

Task	Type	Heads	Layers	T	P	C	N_B	num_trajs
Branin (toy)	Continuous	4	8	64	32	32	32	400
TFBind8	Discrete	8	8	128	64	64	64	800
TFBind10	Discrete	8	8	128	64	64	64	800
D'Kitty	Continuous	8	32	128	64	64	64	800
Ant	Continuous	8	32	128	64	64	64	800
Superconductor	Continuous	8	32	128	64	64	64	800

Table 4: Important parameters for all the tasks

³<https://github.com/karpathy/minGPT>

⁴<https://github.com/kzl/decision-transformer>

B.4 Fixed vs. Updated RB during evaluation

During the evaluation of the prediction sequence, we proposed to keep the Regret Budget (RB) fixed. One alternative strategy is to sequentially update RB after every iteration, i.e. predict \mathbf{x}_t from R_t , and compute $R_{t+1} = R_t - (f(\mathbf{x}^*) - f(\mathbf{x}_t))$. However, there are two issues with such an update rule:

1. Updating RB adds a sequential dependency on our model during evaluation, as we must query $f(\mathbf{x}_t)$ to compute R_{t+1} . Thus, generating the Q candidate points is not purely offline.
2. While updating the regret budget R_t , it is possible that at some timestep t , R_t becomes negative. Since the model has never seen negative RB values during training, this is undesirable.

Hence, we do not update RB during evaluation, and instead provide a fixed \hat{R} value at every timestep after the prefix length. This way, point proposal is not dependent on sequential evaluations of f , making it much faster as the evaluations on f can then be parallelized. Furthermore, by not updating \hat{R} we sidestep the issue of negative RBs. Empirically, as we see in Figure 8, there is not much difference across different strategies, which justifies our choice of not updating RB, allowing our method to be purely offline.

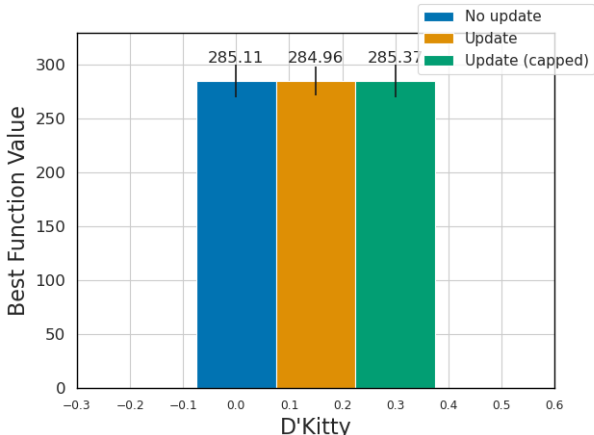


Figure 8: Comparison between 3 strategies: (1) do not update the RB at all (blue), (2) update the RB but do not handle the case when R_t becomes negative (orange) and (3) don't make the update if the update is going to make the RB negative and update otherwise (green). In all three cases, we see similar performance.

B.5 Baselines

For the gradient ascent baseline of Branin task, we train a 2 layer neural network (with hidden layer of size 128) as a forward model for 75 epochs with a fixed learning rate of 10^{-4} . For gradient ascent on the learnt model during evaluation, we report results with a step size of 0.1 for 64 steps. We average over 5 seeds, and for each seed we perform two random restarts.

For the baselines in the Design-Bench tasks, we run the baseline code ⁵ provided in Trabucco et al. [3] and report results with the default parameters for a query budget of 256.

B.6 Design-Bench Tasks

For the Design-Bench tasks, we pre-process the offline dataset to normalize the function values before constructing the trajectory dataset $\mathcal{D}_{\text{traj}}$. Normalized y_{norm} values are computed as $y_{\text{norm}} = \frac{y - y_{\text{min}}}{y_{\text{max}} - y_{\text{min}}}$, where y_{min} and y_{max} are minimum and maximum function values of a much larger hidden dataset. Note that we only use the knowledge of y_{min} and y_{max} from this hidden dataset,

⁵We were not able to reproduce the results of [38] and [22] on the latest version of Design-Bench.

and not the corresponding \mathbf{x} values. With this normalization procedure, we use 1.0 as an estimate of $f(\mathbf{x}^*)$ while constructing trajectories in $\mathcal{D}_{\text{traj}}$. The results we report in Table 2 are also normalized using the same procedure, similar to prior works [3, 8]. We also report unnormalized results in Table 5.

C Additional Experimental Results

C.1 Ablations on SORT-SAMPLE

SORT-SAMPLE algorithm has two main components: Sampling after re-weighting and sorting. In this section, we perform ablations to see the effects of these components. To this end, we construct trajectories using 4 strategies:

1. Random: Uniformly randomly sample a trajectory from the offline dataset.
2. Random + Sorting: Uniformly randomly sample a trajectory from the offline dataset and sort it in ascending order of the function values.
3. Re-weighting + Partial Sorting: Perform re-weighting, uniformly randomly sample n_i number of points from each bin, and concatenate them from lowest quality bin to the highest quality bin. This way, the trajectory will be partially sorted, i.e. the order of the bins themselves is sorted, but the points sampled from a bin will be randomly ordered. In this case, the trajectories are not entirely monotonic w.r.t. the function values. Intuitively, this intermingles exploration and exploitation phases within and across bins respectively.
4. Re-weighting + Sorting (default in BOOMER): Sort the trajectory obtained in strategy 3. This is the default setting we use in our experiments.

Figure 9 contains the results obtained by each of the four strategies. Note that while going from strategy 1 to 2, we keep the points sampled in a trajectory the same, so the only difference between them is sorting. Figure 9 shows that strategy 1 clearly outperforms strategy 2. This means that sorting has a significant impact on the results. Next, note that strategy 2 and 4 differ only in their sampling strategy, and strategy 4 outperforms strategy 2, which shows the effectiveness of re-weighting. This experiment justifies our choice for both re-weighting and sorting.

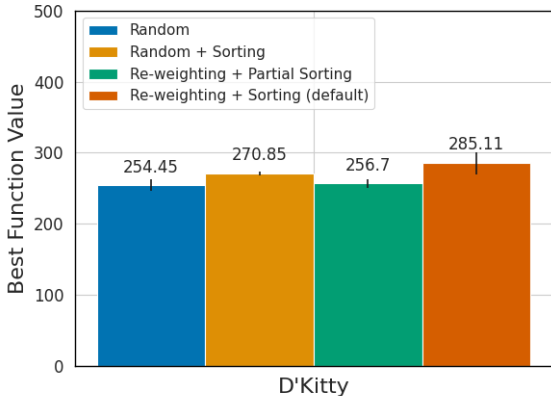


Figure 9: Results with various trajectory construction strategies for D’Kitty task, averaged over 5 runs. Comparing blue and orange bars, it is evident that sorting is improving the results. Similarly, comparison of orange bar with red bar shows that re-weighting further improves the results.

C.2 Analysis on query budget Q

So far, we have been discussing the results with query budget $Q = 256$. Here, we describe the evaluation strategy we use when lower query budget is available. Our strategy will be to give higher preference to lower \hat{R} values when lower budget is available. For example, when $Q = 192$,

we only roll-out and evaluate for $\hat{R} \in \{0.0, 0.01, 0.05\}$. For $192 < Q \leq 256$, we will roll-out for $\hat{R} \in \{0.0, 0.01, 0.05, 0.1\}$, evaluate the entire predicted sub-sequences of lengths 64 for $\{0.0, 0.01, 0.05\}$, and evaluate the first $Q - 192$ points in the predicted sub-sequences for $\hat{R} = 0.1$. In the Figure 10, we present the results for different query budgets for our method compared to important baselines, for the D’Kitty task. We outperform the baselines for almost all the query budget values.

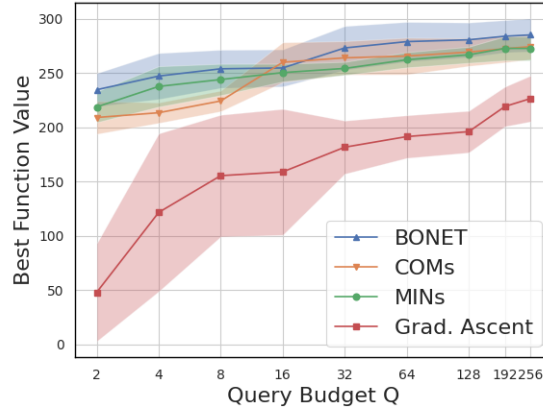


Figure 10: Results for various query budget values Q for D’Kitty task, averaged over 5 runs. We match or outperform other baselines on almost all the values of Q .

C.3 Additional Ablations

Here we present ablations similar to Section 3 on the D’Kitty task, and observe similar trends to what we see in the Branin ablations.



Figure 11: Figures 11a and 11b show plots of the trajectories generated on DKitty for different values of evaluation RB (0, 8 and 10). In Figure 11a we show results without updating RB, and in Figure 11b we show results with updating. All the trajectories are averaged over 5 runs.

D Societal Impact

Offline black-box optimization can play a critical role in improving efficiency and safety in many real world settings like in nuclear reactors or in the pharmaceutical industry where active optimization may prove to be computationally inefficient (requiring too many queries) or even dangerous. However, while we do not anticipate anything inherently malicious about our work, it is possible to utilize our

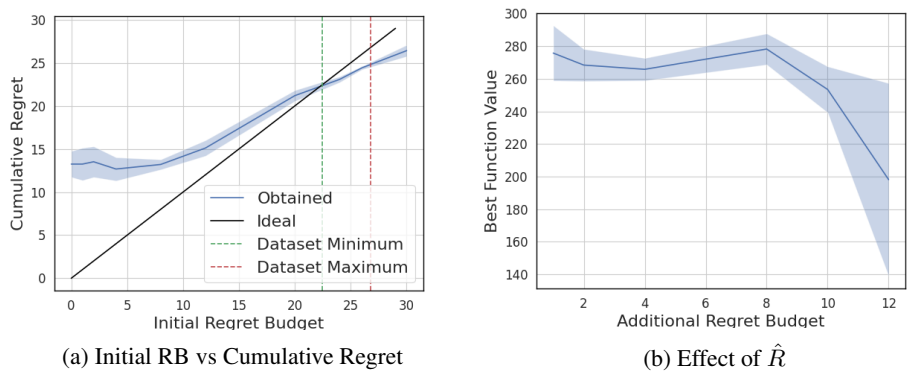


Figure 12: Ablations on D’Kitty, averaged over 5 runs.

Baseline	TFBind8	TFBind10	Superconductor	AntMorphology	D’Kitty Morphology	ChEMBL	NAS
CbAS	0.958 ± 0.018	0.761 ± 0.067	83.178 ± 15.372	468.711 ± 14.593	213.917 ± 19.863	388996.000 ± 731.011	66.360 ± 0.820
BO-qEI	0.824 ± 0.086	0.675 ± 0.043	92.686 ± 3.944	480.049 ± 0.000	213.816 ± 0.000	387962.590 ± 0.000	69.722 ± 0.606
CMA-ES	0.933 ± 0.035	0.848 ± 0.136	90.821 ± 0.661	1016.409 ± 906.407	4.700 ± 2.230	388402.719 ± 622.401	69.475 ± 0.821
Gradient Ascent	0.981 ± 0.010	0.770 ± 0.154	93.252 ± 0.886	-54.955 ± 33.482	226.491 ± 21.120	389978.375 ± 2965.207	63.770 ± 0.000
REINFORCE	0.959 ± 0.013	0.692 ± 0.113	89.027 ± 3.093	-131.907 ± 41.003	-301.866 ± 246.284	388332.156 ± 369.562	39.720 ± 0.000
MINs	0.938 ± 0.047	0.770 ± 0.177	89.469 ± 3.227	533.636 ± 17.938	272.675 ± 11.069	391016.281 ± 3400.081	66.709 ± 0.471
COMs	0.964 ± 0.020	0.750 ± 0.078	78.178 ± 6.179	540.603 ± 20.205	277.888 ± 7.799	390223.500804.333	64.041 ± 1.431
BOOMER	0.975 ± 0.004	0.855 ± 0.139	80.84 ± 4.087	567.042 ± 11.653	285.110 ± 15.130	391171.4122891.088	66.780 ± 0.086

Table 5: Unnormalized results with 256 query budget

proposed method (and other optimizers in general) in malicious settings (e.g. for optimizing for drugs that have harmful effects). This is something to keep in mind when deploying algorithms such as ours for high stake real-world applications.